ORIGINAL PAPER

Morphological study of bronchial mucosa in the chronic obstructive pulmonary disease under the influence of therapeutic algorithm

Gh. Nini[1], M. Raica[2], V. Neamţiu[3], M. Onel[3]

[1]Clinical Department of Pneumology,
"Vasile Goldiş" Western University, Arad
[2]Department of Histology and Cytology,
"Victor Babeş" University of Medicine and Pharmacy, Timisoara
[3]"Vasile Goldiş" Western University, Arad

Abstract

Objectives: Immunohistochemical evaluation of the effectiveness of bronchodilator treatment in patients with chronic obstructive pulmonary disease (COPD). *Materials and Methods*: There have been examined bronchial mucosa biopsies taken endoscopically from 18 patients with obstructive pulmonary disease. The biopsies were fixed in 4% buffered formalin for 24–48 hours and paraffin inclusion was made using the standard technique. For each biopsy, there were performed 10 serial sections with a thickness of 5 μm. The sections were stained using morphological, histochemical and immunohistochemical methods. At three of the cases, the paraffin blocks were reconverted for the electron microscopy study, in order to assess subcellular details, with special reference to "target" cells involved in local immune response. Morphohistochemical and immunohistochemical analysis was effectuated on biopsies removed before and after the treatment with bronchodilators. *Results*: The analysis of the biopsies removed before treatment revealed the following aspects: degenerative alterations of the surface epithelium, loss of ciliary differentiation, absence of caliciform cells, hyperexfoliation, formation of pseudopapillary structures, degenerative lesions of the glands, mucoid and oncocytary metaplasia, stasis in the dilated blood vessels, partly hyalinized wall, multiforme chronic inflammatory infiltrate, myofibroblasts in the depth of lamina propria; argyrophilic basement membrane, fragmentation and lysis of elastic fibers, degranulated mast cells associated with inflammatory infiltrate, with electron-dense typical granules, inflammatory infiltrate with CD20 positive B-lymphocytes, arranged perivasculary and in the vicinity of the basement membrane; rare positive CD4 T-lymphocytes; reduced number of plasma cells. After treatment we found the following aspects: partial or complete regeneration of the covering epithelium, with the presence of cilia cells and occasionally of caliciform cells; remaining myofibroblastic reaction in the lamina propria; increased number of mast cells with minimal or no degranulation; immature, lamelled mast cells. *Conclusions*: The application of management principles in group therapy study was done by the study which aims to demonstrate the beneficial role in COPD therapy of combining a β2-agonist with an anticholinergic, obtaining in this way an additional bronchodilator effect, compared with the one obtained by administrating bronchodilators of type β2 agonists. Deepening the molecular and cellular mechanisms of COPD can lead to more effective methods for early detection of disease, pharmacotherapy targeted and effective conduct exacerbations.

Keywords: chronic obstructive pulmonary disease, bronchial mucosa, inflammatory infiltrate, mast cells, CD68.

⊟ Introduction

Medicine registers significant progress reflected in increasing life expectancy and lower overall population morbidity, because of combining the work of health professionals with clinical activity research. However, there are several affections that know an increasing trend in prevalence, chronic obstructive pulmonary disease (COPD) belonging to this category too.

It can be said that chronic obstructive pulmonary disease is an inflammatory disease that affects both the aeriferous ducts and the lung parenchyma in which, at predisposed individuals, external aggressors (mainly cigarette smoke) trigger an "aggressive" cascade in which neutrophil and its products play an essential part [1].

Currently, there is a tendency all over the world towards a unified approach to chronic obstructive pulmonary pathology reporting given the upward evolution of the prevalence of this group of diseases: it is estimated that by 2020 COPD will be the fourth cause of mortality [2, 3]. These statistical estimates overlap with current trends in what concerns risk factors: increasing air pollution [4], increasing incidence of smoking in females [5], ageing.

At the annual congresses of the *European Respiratory Society* (ERS) and of the *American Thoracic Society* (ATS) the importance of COPD was outlined even more significantly, as well as major differences from asthma at the molecular level, leading to increased investment in research and developing clinical guidelines for COPD [6]. The most controversial aspects in literature are related to several issues:

▪ Susceptibility of only 15–20% of smokers to develop the disease;

▪ Predisposition to heart diseases or lung cancer of those with bronchial obstruction;

▪ Predilection for the prophylactic or curative side;

▪ Cost-benefit efficiency of the treatment to improve the symptoms and the quality of life;

▪ The existence of different classification criteria.

At the current level of knowledge, it can be stated that chronic obstructive pulmonary disease is a controllable disease by creating on international level, at the initiative of the *U.S. National Heart, Lung and Blood Institute* and *World Health Organization* of the GOLD programme – *Global Initiative for Chronic Obstructive Pulmonary Disease* [7].

This has resulted in the publication of a practical guide to diagnosis, prevention and management of COPD. COPD management between exacerbations is based in terms of pathophysiology on achieving and maintaining a balance between the determinants of respiratory failure and compensation factors [8]. This goal constitutes the physiopathological prerequisite of a rational therapy.

The importance of the problem

Bronchospasm characterizes a large part of patients with chronic obstructive pulmonary disease. Reversible obstructive syndrome is generated in the vegetative nerve sparing of the bronchial smooth muscle and can be combated, annihilated through bronchodilator medication. In initiating the inhaled bronchodilators therapy in chronic obstructive pulmonary disease, the clinical, paraclinical and immunohistochemical evaluation are important steps.

The cost-efficiency report calls for an interactive management of COPD treatment, in which the information and training of the patient in order to support the cooperation with the doctor represents the key to success, being supported by clinical, paraclinical and immunohistochemical evaluation.

The patient should know his disease, should learn how to participate in the treatment and when to be alarmed, these being indispensable prerequisites for the physician–patient cooperation [9].

Objective

Evaluation through immunohistochemical methods of the effectiveness of bronchodilator therapy in COPD.

⊟ Materials and Methods

Bronchial mucosa biopsies taken endoscopically from 18 patients with obstructive pulmonary disease were studied. Biopsies were fixed in 4% buffered formalin for 24–48 hours and paraffin inclusion was made using the standard technique. For each biopsy 10 serial sections with a thickness of 5 μm were performed. The sections processed in this way were stained using morphological, histochemical and immunohistochemical methods. In three of the cases, the paraffin blocks were reconverted for the electron microscopy study, to assess subcellular detail, with special reference to "target" cells involved in the local immune response.

Morphological methods

▪ Hematoxylin–Eosin, standard technique, through which were revealed basic lesions on bronchial biopsies.

▪ Masson trichrome staining, which evidentiates in blue-violet the nuclei, in red the muscle cells and in blue the collagen fibers and the hyalinisation areas.

Histochemical methods

▪ Coloration with Toluidine Blue, at pH 4.2, for the overall identification of glycosaminoglycans and mucin-secreting cells, through the metachromasia and orto-chromasia phenomena.

▪ Coloration with Alcian Blue–Safranin, at pH 0.2, in order to identify the mast cells which contain in specific granules high sulphate glycosaminoglycans of the heparin and chondroitin sulfate type; the method was particularly useful for identifying the dominant type of glycosaminoglycan form the mast granules on the one hand and assessing the degree of degranulation on the other hand.

▪ Gordon–Sweet type silver impregnation, in order to highlight the basal membranes.

▪ Coloration with Orcein, Unna–Tänzer method, specific to the elastic fibers that occur in all the structures of the bronchial wall.

Immunohistochemical methods

▪ Specific methods have been applied in order to identify the components of the inflammatory infiltrate (subtypes of lymphocytes, macrophages).

▪ The working system used was LSAB2 (labeled Streptavidin–Biotin).

▪ Chromogen was represented in diaminobenzidine dihydrochloride so that the final reaction product was colored brown.

▪ The endogenous peroxidase was inhibited with 3% hydrogen peroxide.

▪ Antigen unmasking was performed in the micro-wave for 20 minutes in citrate buffer (pH 6).

▪ Nuclear counterstaining with modified Lillie's Hematoxylin.

▪ The whole procedure was effectuated with Dako's Autostainer.

▪ The antibodies used were the following:

− Anti-vimentin, clone V9, which identifies inter-mediate filaments specific to mesoderm cells;

− Anti-LCA (common leukocyte antigen), which marks an epitope on the leukocyte membrane: method proved useful for assessing inflammatory density before and after treatment;

− Anti-CD20, which identifies a surface membrane antigen-specific to B-lymphocytes and is negative for all T-lymphocytes;

− Anti-CD3, CD4 and CD8, which identify different subtypes of T-lymphocytes, and also recognize a membrane antigen; the three methods are negative for B-lymphocytes;

− Anti-CD68, specific for macrophages and has granular cytoplasmic distribution.

Optical microscopy images were acquired as a JPEG file and the image analysis on the density of inflammatory infiltrate was assisted by LUCIA G Nikon programme.

Processing for electron microscopy specimens consisted of dewaxing reconversion, post-fixing with 1% osmic acid.

Fragments chosen after examining the preparations stained using routine methods were inclusionated in

Epon812, sectioned at ultramicrotome and contrasted with lead citrate and uranyl nitrate. Electron microscope examination was performed with Zeiss–Leica LEO906.

⊟ Results

In order to highlight the structural changes before and after treatment we used at a number of 18 cases the morphological, histochemical and immunohistochemical study of the biopsies taken by fibrobronchoscopy. There were used histochemical and immunohistochemical methods, morphohistochemical and immunohisto-chemical analysis being performed on biopsies taken before beginning the treatment and after the treatment with bronchodilators.

Primary morphological evaluation on sections stained with Hematoxylin–Eosin revealed significant differences between biopsies taken from the same patients before and after treatment. These changes are relevant for the mucosal epithelial component (coating and glandular epithelium), as well as for the conjunctive component. The only component that showed no significant morphological changes was the muscle component.

In untreated cases, severe mucosal lesions, present in all components, were observed.

The covering epithelium showed significant morphological changes in all cases. They were characterized by the loss of the pseudostratified character, so that cells with cilia were no longer identified in most cases. In addition, the cellular heterogeneity that can be found in normal respiratory epithelium type was absent. Simultaneously, we noted extensive areas of epithelial denudation, alternating with areas of flat epithelium (Figure 1).

The flat epithelium consisted of cells with mono-morphic aspect, with eosinophilia cytoplasm, nucleus intensely colored and size variations from one cell to another. Frequently, from the areas of degenerated epithelium a massive exfoliation of skin cells was observed. Basement membrane was significantly thickened, acidophilous. In the lamina propria of the mucosa we noticed at five cases suffusions bleeding, mixed with inflammatory cells. The inflammatory cells were arranged close to the basement membrane and hemorrhagic areas were stationed in the deep portion of lamina propria (Figure 2). Aspects of this type with the highest intensity were noted in cases with severe alterations of epithelial coverage.

A particular aspect was observed in three cases, where we noted the epithelial proliferation of pseudo-papillary type, characterized by focal stratification of epithelial cells (Figure 3). The presence of these epithelial proliferations signals the regenerative focal nature of bronchial epithelium. For this reason, we can assume that many of the reshuffle epithelial cells are basal.

Glandular changes were observed in all cases included in the study. On the one hand, we mention the disappearance of the caliciform cells, due to degenerative lesions of surface epithelium. On the other hand, we noticed the hypertrophy of glands from the lamina propria.

We observed three types of glandular lesions: mucinous metaplasia, focal necrosis and oncocytary metaplasia. Normal bronchial mucosa contains predo-minantly serous and mixed glands, whose secretory units are small. In the cases we studied, we observed the marked hypertrophy of the acini and their transfor-mation in the meaning of mucin secretion. Because of this, on the histological sections, the acini were large, with wide lumen and the secretory cells had pale cytoplasm with the usual methods, hyperchrome nuclei (Figure 4).

Unlike "classical" mucous acini, the ones of mucous metaplasia are characterized by cells with randomly disposed nuclei and not at the basal pole. Mucoid metaplasia of the glands explains the mucoid hyper-secretion clinically observed in patients with COPD.

In some groups of acini, a blurring of boundaries between neighboring cells was noted, which indicates necrosis (Figure 5) – consecutive to the stasis usually observed in most cases.

We found oncocytic metaplasia in five cases. Oncocytes are glandular cells, with intensely acidophilous cytoplasm due to the great number of mitochondria. Although they are reported as isolated cells and in normal conditions present at elderly persons, in patients we identified them, they were concentrated in the form of small groups in the glandular units (Figure 6). The significance of the oncocytes is uncertain, both in normal and pathological conditions. We consider that the oncocytic hyperplasia observed in COPD reflects an adaptive response of the glandular cells to tissue hypoxia that occurs in these conditions.

All cases morphologically investigated showed an abundant inflammatory infiltrate before treatment. The infiltrate was polymorphic in all cases, which were mostly lymphocytes and macrophages. Rarely, we observed neutrophilic granulocytes, eosinophils and only exceptionally plasma cells. Macrophages attracted attention in most cases, many of which had black inclusions in the cytoplasm, being similar form this point of view to dusty cells observed in lung parenchyma (Figure 7).

Inflammatory infiltrate could be easily differentiated from the bronchial mucosa-associated lymphoid tissue due to heterogeneous nature of the cellularity and to the fact that it was not organized as a lymphoid tissue. On the other hand, mucosa-associated lymphoid tissue in humans is poorly represented and it is located mainly in the bronchial mucosa in the form of small follicles. Frequently, the infiltrate was located in the immediate vicinity of the dilated blood vessels, and in the post-capillary venules we noticed an intense process of leukocyte margination (Figure 8).

The leukocyte margination correlates with the high-density of inflammatory cells from the mucosal tissue. The density per area unit of the inflammatory infiltrate significantly reduces in the deep portion of the lamina propria, so that near the muscular layer are observed only rare isolated lymphocytes (Figure 9). On the other hand, in this area we found an intense tissue reaction,

reflected by the appearance of stellate shaped cells with branched extensions that establish contacts with neighboring cell. These cells have an indented nucleus, hyperchrome, acidophilous cytoplasm and have been highly positive to the immunoreaction for smooth muscle actin type (Figure 10).

According to these morphological and immunohisto-chemical characteristics these cells were classified as myofibroblasts.

Under normal conditions, myofibroblasts are absent from the bronchial wall structure. Their presence in a large number in the investigated cases indicates the existence of a scar-type repair process, as seen in other parts of the body under conditions of chronic inflammatory diseases.

Another structural feature remarked on the inflammatory infiltrate consists of preferential disposal of lymphocytes around small blood vessels, highly branched (Figure 11).

These vessels have very thin wall and form a true network across the lamina propria area occupied by lymphocytes. For this reason, it is often difficult to observe the preparations stained with the help of routine methods but it is easily visualized with specific immuno-reactions for von Willebrand factor (Figure 12).

The presence of numerous blood vessels associated with the inflammatory infiltrate raises the question of the existence of an angiogenesis process concomitant with the inflammation. For this reason, we focused the following morphological observations on blood vessels in the bronchial mucosa.

The first aspect that attracts attention, from this point of view, when examining with a small objective, refers to the presence of a large number of blood vessels with wide lumens and stasis aspect (Figure 13).

All these vessels have thin walls, containing a large number of red cells in the lumen and are located in the superficial half of the lamina propria (Figure 14).
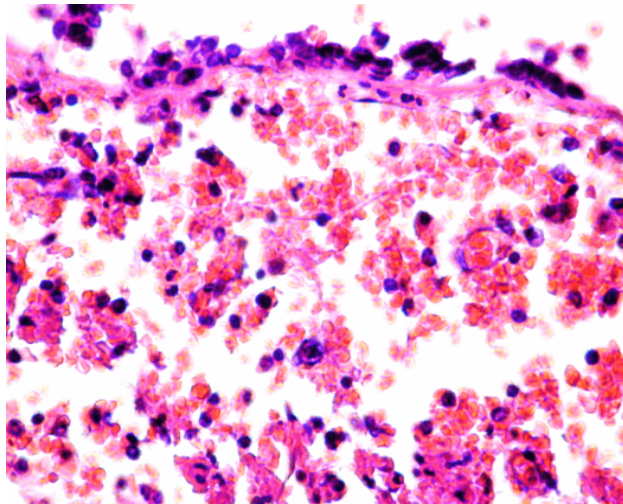
Figure 1 – *Atrophic epithelium type, denuded, with hyperexfoliation (HE stain, ob. ×20).*
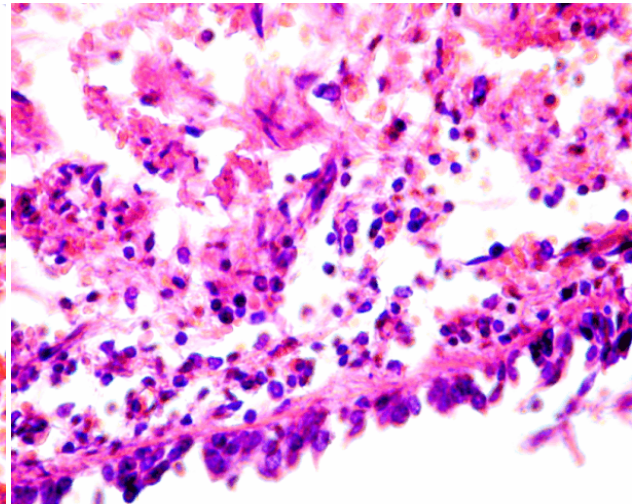
Figure 2 – *Covering epithelium with severe degenerative changes, thick basement membrane, inflammatory infiltrate in the superficial portion of the lamina propria and in-depth hemorrhagic suffusion (HE stain, ob. ×20).*
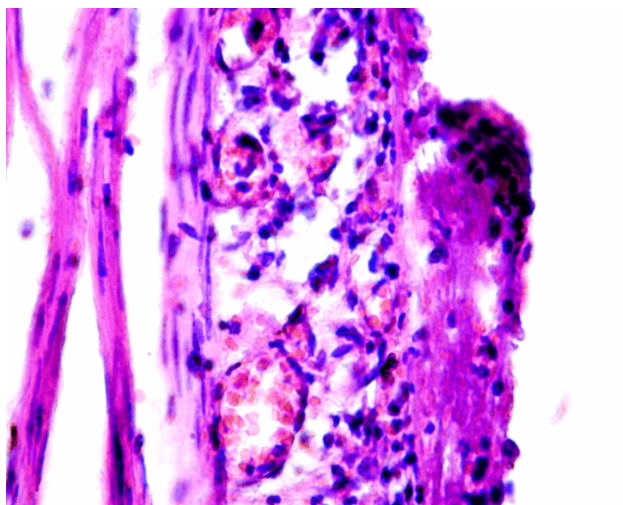

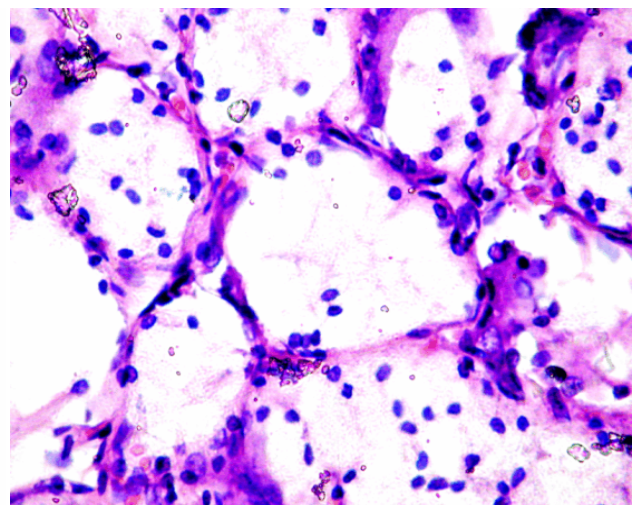**Figure 3** – *Focal epithelial proliferation of pseudo-papillary type (HE stain, ob. ×20).*

Figure 4 – *Acini of mucoid metaplasia, of large dimensions, with wide lumen and cells with clear cytoplasm showing hyperchrome nucleus (HE stain, ob. ×20).*
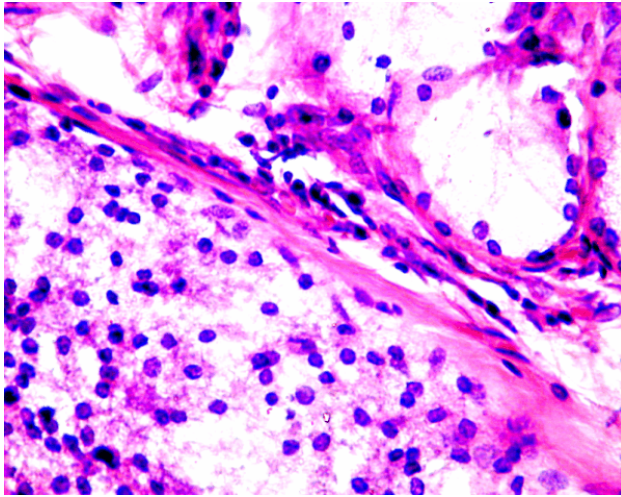
Figure 5 – *Mucus-secreting glands with the aspect of mucoid metaplasia (upper right) and glands with necrosis (bottom left), which is observed at the boundaries between neighboring cells (HE stain, ob. ×20).*
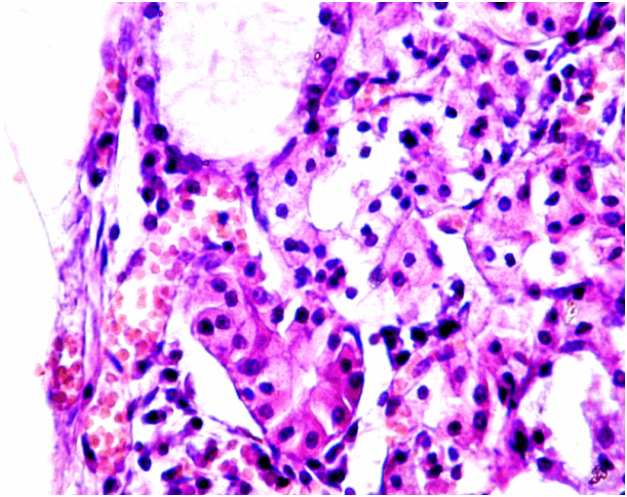

Figure 6 – *Oncocytic metaplasia, with cells that have lost their secretory character and have the cytoplasm intensely stained granular with eosin (HE stain, ob. ×20).*
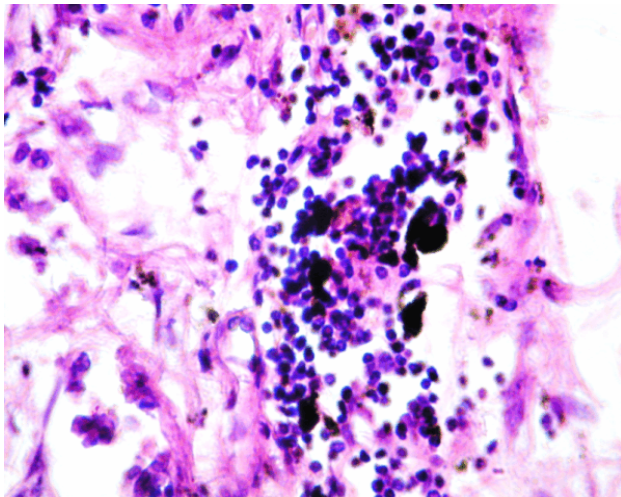

Figure 7 – *High-density cell inflammatory infiltrate located in the lamina propria of mucosa, composed of lymphocytes and macrophages with inclusions (HE stain, ob. ×20).*
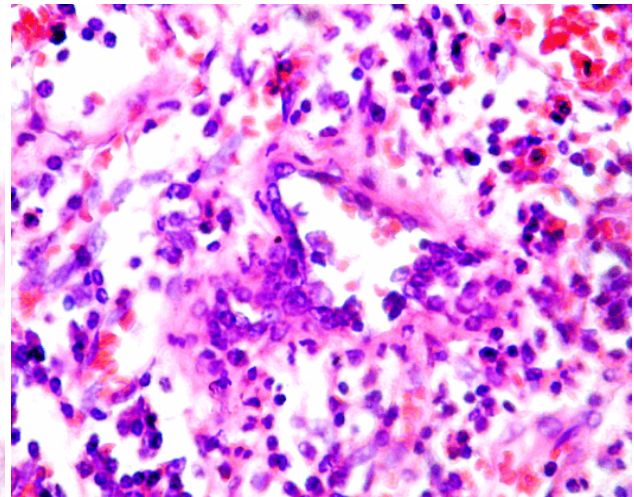
Figure 8 – *Perivascular polymorphous chronic inflammatory infiltrate associated with leukocyte margination (HE stain, ob. ×20).*
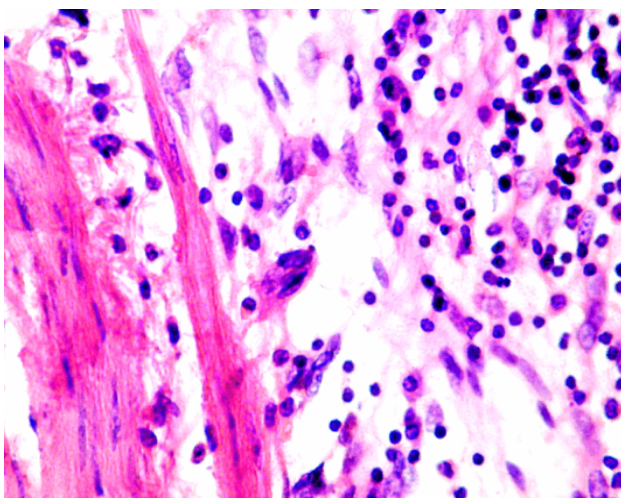
Figure 9 – *Decrease in the density of chronic inflammatory infiltrate in the deep region of the lamina propria. Presence of cells with myofibroblastic morphology (HE stain, ob. ×20).*
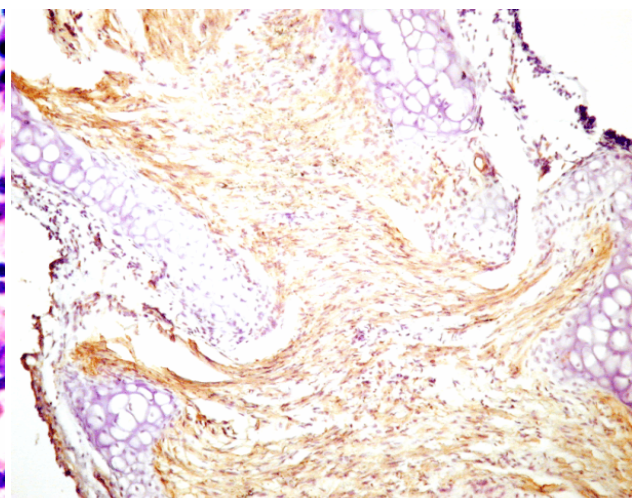
Figure 10 – *Intense reaction for smooth muscle actin type in the deep portion of the lamina propria (ob. ×10).*
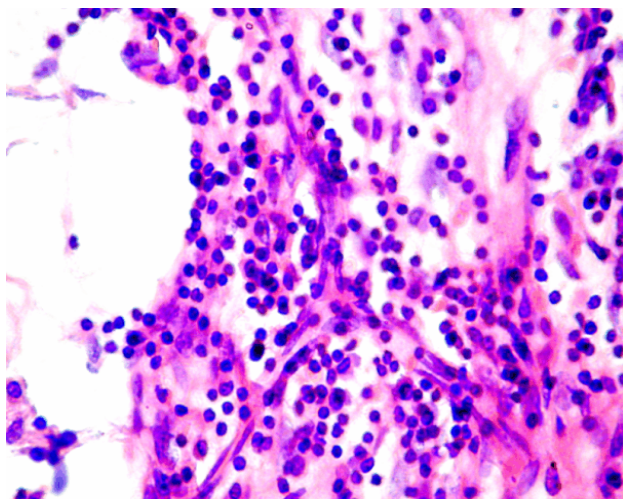
Figure 11 – *Inflammatory infiltrate with high-density composed predominantly of lymphocytes concentrated around a branched blood vessel, with narrow lumen and thin wall (ob. ×20).*
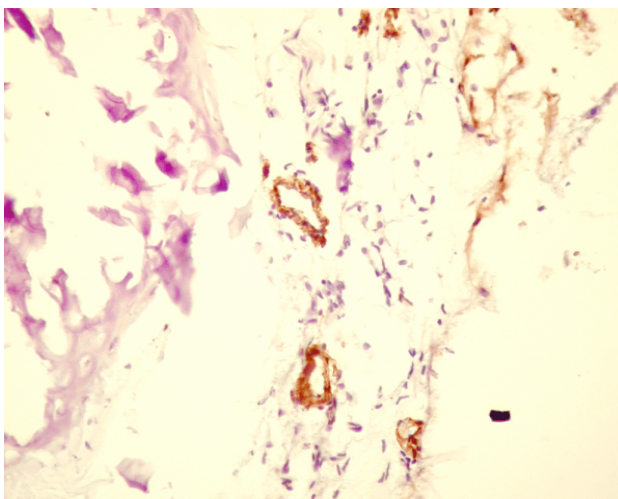

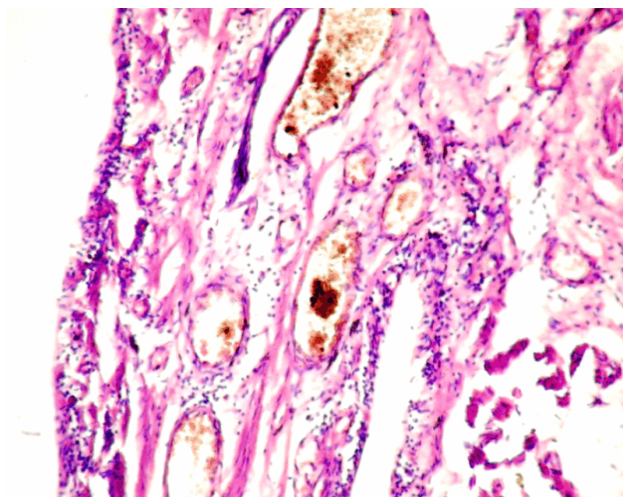**Figure 12 – *Endothelium of blood vessels marked with von Willebrand factor (ob. ×20).***

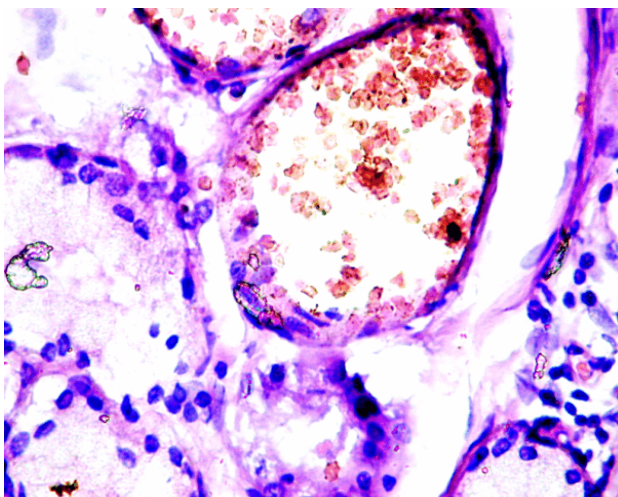**Figure 13 – *Numerous stasis blood vessels located in the lamina propria (HE stain, ob. ×20).***

Figure 14 – *Thin-walled blood vessel and marked stasis (HE stain, ob. ×200).*

Most blood vessels have hyalinisation focal areas, and partial loss of smooth muscle cells from the average.

On the other hand, we found the presence of a process of addition of new cells to the vascular wall on its external side (Figure 15), which leads to global thickening and hyalinization.

On biopsies taken from treated patients, we observed significant morphological changes to the initial biopsy in eight cases. Just like in the initial biopsies, we watched the aspects of the epithelium, of the lamina propria and of the blood vessels. After treatment, we observed the reconstitution of the respiratory type pseudostratified epithelium in five cases (Figure 16).

Restoration was not complete because the vast majority of cells were of ciliated columnar type and only few caliciform cells were present, although at this level they should represent approximately 25% of the cells.

The reconstruction of the surface epithelium was of ciliated pseudostratified type. At the apical pole of columnar cells can be noticed the accentuation of acidophily and the presence of numerous microvilli.

In the lamina propria, is missing a well-established inflammatory infiltrate, mobile cells are isolated, distant from each other. The differentiation of columnar cells was almost complete because at most of them the apical area with pronounced acidophily, which signalizes the presence of cilia, was observed. The basement membrane was significantly thinner than before the treatment, aspect demonstrated by the positivation of the Gordon–Sweet reaction (Figure 17).

Basement membrane was present in all cases, aspect demonstrated by the positive reaction to silver impregnation. Its presence represents the support for the regeneration of the epithelium and possibly for the abnormal, pseudopapillary type proliferation.

Although the basement membrane was present, intensely argyrophil of linear type, we did not observe epithelial regeneration in two cases (Figure 18). We noticed stasis only occasionally, in small vessels in the immediate vicinity of the epithelium (Figure 19).

In some cases, we observed the quasicomplete remission of inflammatory infiltrate, lamina propria being without aggregates of lymphocytes and macrophages (Figure 20).
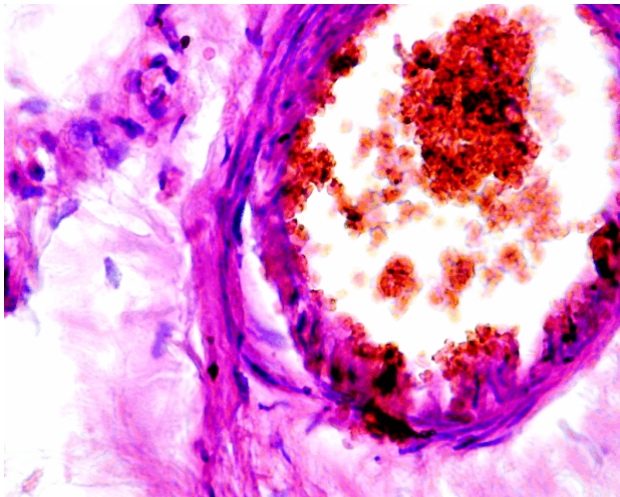
Figure 15 – *Blood vessel around which spindle connective elements are concentrated which lead to wall thickening and hyalinisation (HE stain, ob. ×200).*
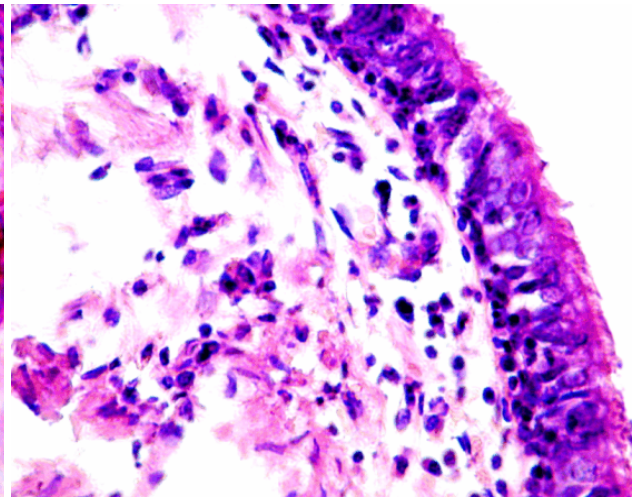

Figure 16 – *Mucosal aspect of post-treatment cases (HE stain, ob. ×20).*
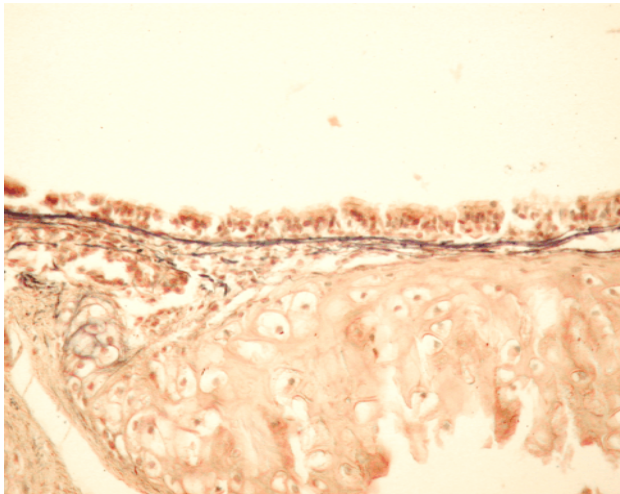

Figure 17 – *The argyrophil basal membrane after treatment. There can be noticed a linear disposition at the interface between the epithelium and lamina propria. Reaction Gordon–Sweet silver impregnation (ob. ×20).*
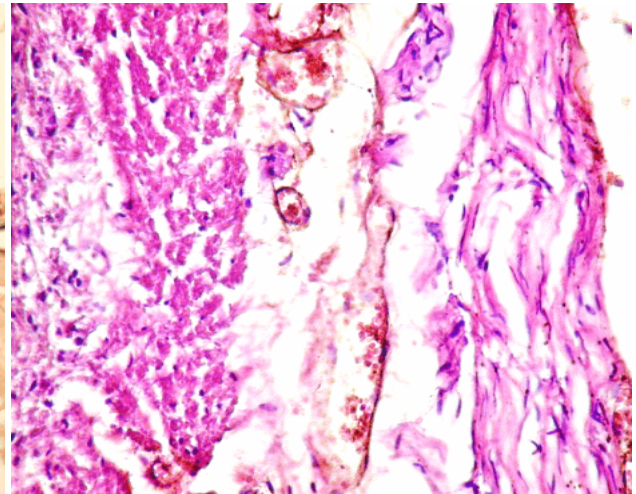

Figure 18 – *Denuded epithelium, basement membrane present, no inflammatory infiltrate in the lamina propria (HE stain, ob. ×20).*
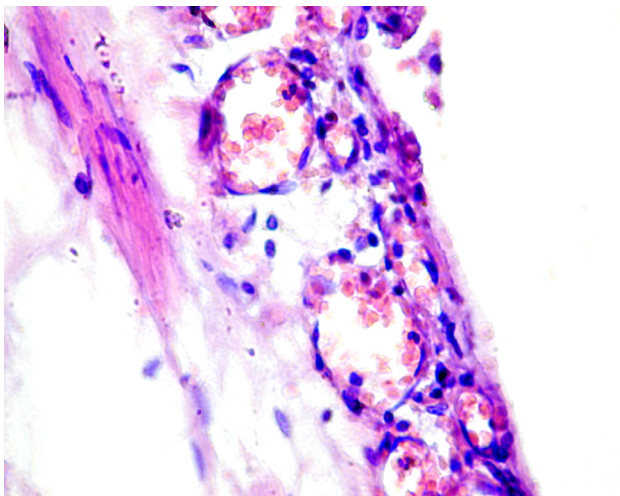

Figure 19 – *Residual stasis in small vessels of the superficial lamina propria, in the absence of inflammatory infiltrate (HE stain, ob. ×20).*
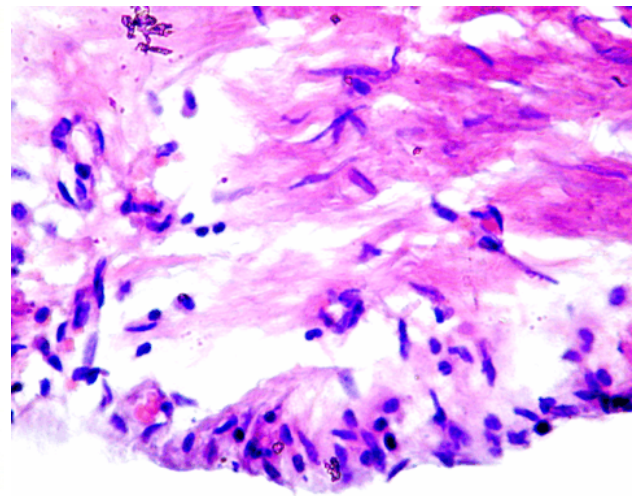

Figure 20 – *Bronchial mucosal biopsy after treatment, with complete remission area in terms of inflammatory infiltrate, the absence of stasis and persistence of myofibroblastic cell types (HE stain, ob. ×20).*

The stasis from the level of blood vessels was also absent and we did not observe interstitial suffusions. Only myofibroblastic cell types persist, causing scar-healing type.

In only one case, we observed normal looking bronchial mucosa after treatment, presenting all the defining elements of the organ (Figure 21).

Another particular aspect that we observed in treated cases refers to the presence and disposition of elastic fibers. We evidentiated the elastic fibers by Orcein reaction and they were colored brown. After the treatment, only four cases (all with no inflammatory infiltrate in the lamina propria) showed elastic fibers in the lamina propria of the mucosa (Figure 22).

In cases with residual inflammatory infiltrate, elastic fibers were absent (Figure 23).

In the same cases, we noted the presence of the myofibroblasts, suggesting that at least some of the basic lesions observed are irreversible.

The study approach of the chronic inflammatory infiltrate has a high degree of difficulty, because of the polymorphic character mentioned above.

On preparations stained with routine morphologic methods it is possible a precise identification only of eosinophilic and neutrophilic granulocytes (Figure 24), due to cytoplasmic nucleotide-specific characters.

It is possible to identify lymphocytes, but we cannot issue assumptions on the subtype of lymphocytes based on morphological observations.

For this reason, we considered appropriate to present separately the cellularity of the inflammatory infiltrate, with particular reference to lymphocytic, macrophagic and mastocytary reaction. Also, the macrophage may be suspected because of the acidophilous character of the cytoplasm (in the absence of inclusions).

Mast cells were present in all cases, both in biopsies taken before, as well as after the treatment. They are medium-sized cells with variable shapes, conferred by numerous cytoplasmic extensions. Typically, at all of them, metachromatic granules were identified.

In the cases biopsied before the treatment, more than 90% of mast cells showed degranulation with different degrees of intensity (Figure 25). These granules are evident both in the cytoplasm of mast cells, as well as in the pericellular space (Figure 26).

The presence of granules in the pericellular space reflects massive degranulation with release of large amounts of biologically active substances.

It is note that in most cases the degranulated mast cells were located in the middle of the inflammatory infiltrate, aspect explained by the cooperation between different cellular elements of the cellular immune response.

Occasionally we noticed mastocytosis aspects, characterized by loss of all cytoplasmic granules, which can be observed only as small metachromatic formations located in the fundamental substance (Figure 27).

Because of the sequential degranulation processes and mastocytosis, mast cell number was significantly lower after treatment than before treatment. The counting of mast cell using the "hot spot" method revealed an average of three mast cells per microscopic field when increasing ×200 (reflecting an area of 0.63 mm^2).

These aspects were confirmed ultrastructurally. In the electronic microscopy effectuated from the same cases, we discovered many mast cells intensely degranulated.

We specify that all these mast cells had uniform granulations, intensely electron-dense, which reflects their mature nature (Figure 28).

In biopsies taken from treated patients, mast cells were present with an average density of 9/microscopic field ×200 magnification. Over 90% of them were orthochromatic and safraninophilic, being weak or not degranulated at all (Figure 29).

Limited degranulation is observed in normal conditions too, but these mast cells are usually alcianophilic. In cases without significant inflammatory infiltrate, in the lamina propria we have noted the accumulation of large numbers of mast cells without degranulation – on average 15–20/field (Figure 30).
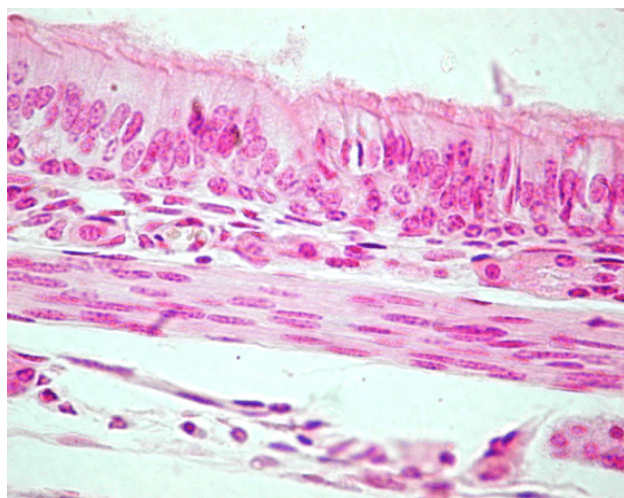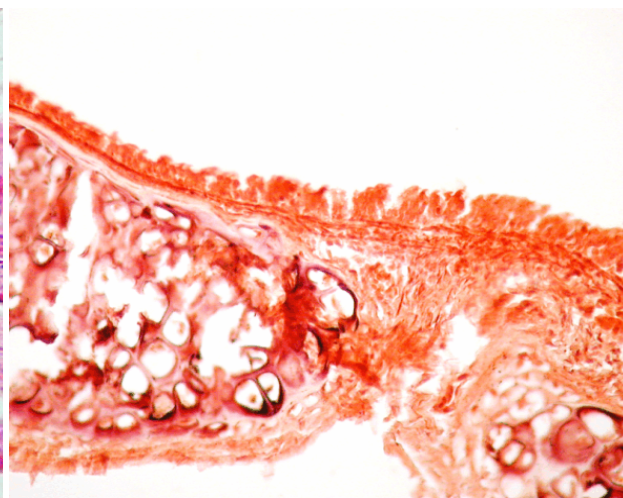

Figure 21 – *Bronchial mucosa of normal type, presenting respiratory type epithelium with ciliary cells, caliciform, without inflammatory elements in the lamina propria and continuous muscle lamina (ob. ×20).*

Figure 22 – *Elastic fibers present in the superficial portion of the lamina propria (Orcein stain, ob. ×20).*
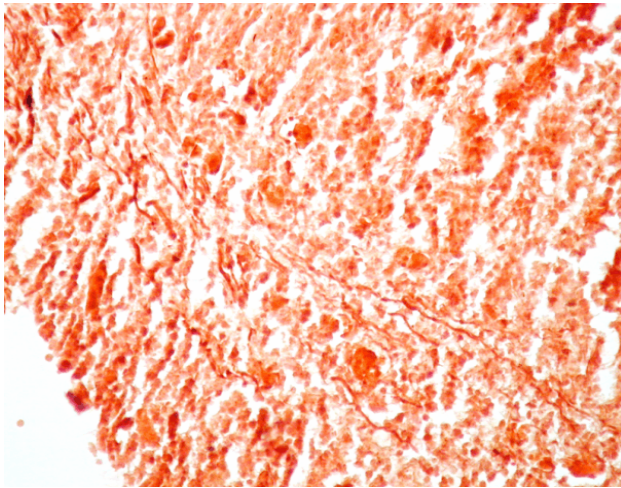
Figure 23 – *Elastic fibers absent in areas with residual inflammatory infiltrate (Orcein stain, ob.×20).*
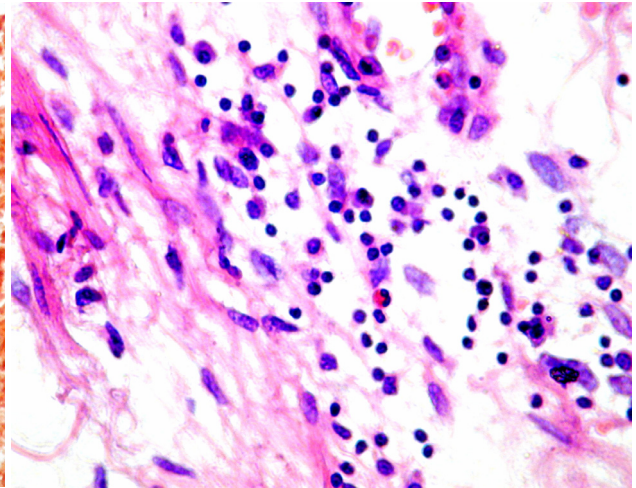

Figure 24 – *Polymorphous inflammatory infiltrate composed of lymphocytes, eosinophilic granulocytes (rare, central position in the image), rare plasma cells and macrophage cell types (HE stain, ob. ×20).*
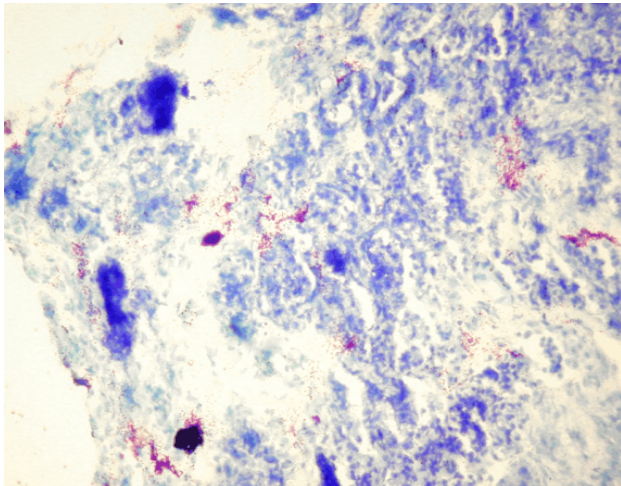

Figure 25 – *Metachromatic mast included in the chronic inflammatory infiltrate (ob. ×200).*
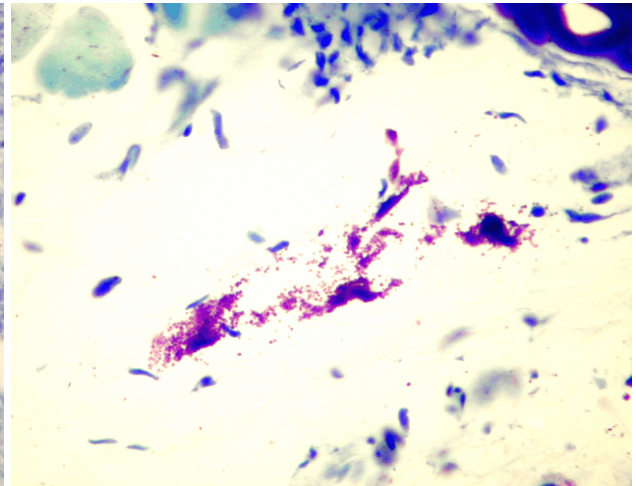

Figure 26 – *Mast cells with metachromatic granules and sequential degranulation. Numerous granules from the pericellular space can be noticed (Toluidine Blue stain, pH 4.2, ob. ×20).*

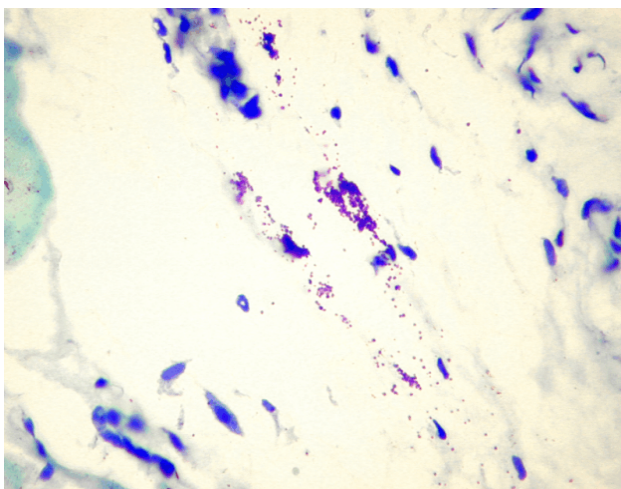**Figure 27 – *Mastocytosis. Aggregates of granules in the fundamental substance (ob. ×20).***
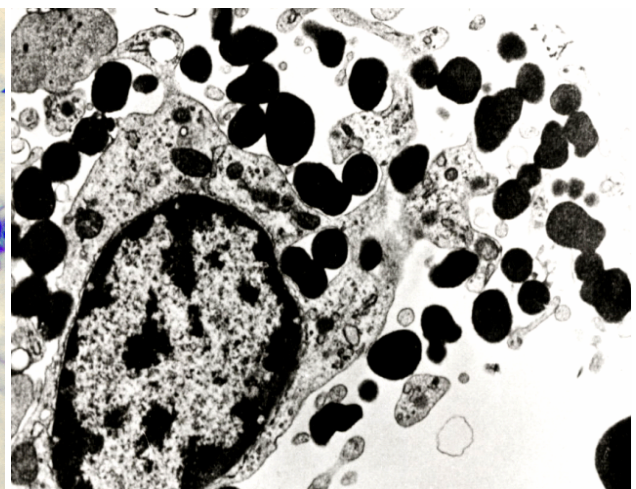

Figure 28– *Mast with mastocytosis. The vast majority of mast granules, homogeneous, intense electron-dense are located in the pericellular space and in cytoplasmic "bags" that communicate with the pericellular space. In the remaining cytoplasm, there are very few non-specific organelles. Electron microscopy, ×42 000.*
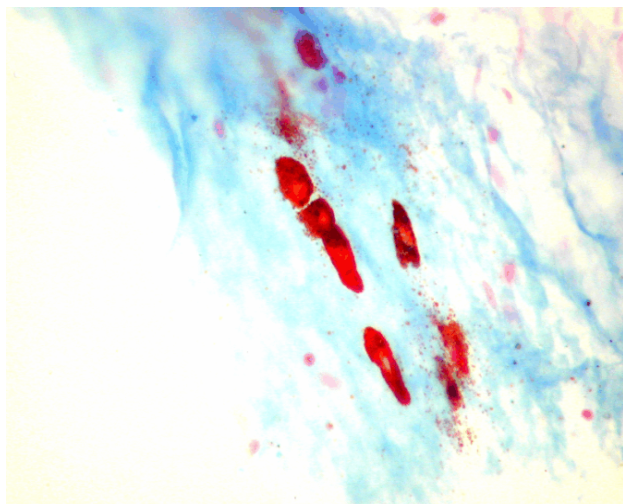
Figure 29 – *Intensely safraninophilic mast cells with minimum degranulation (9 mast cells in a field, ×200). Alcian Blue–Safranin staining.*
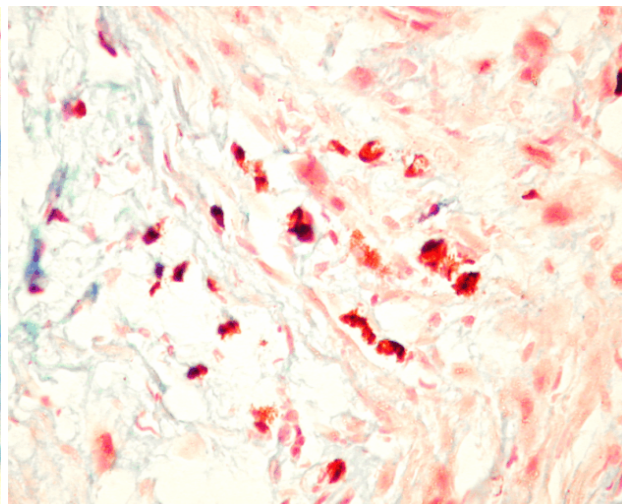

Figure 30 – *Accumulation of safraninophilic mast cells without degranulation in a case without chronic inflammatory infiltrate (ob. ×20).*

Ultrastructurally, these mast cells showed granules with lamellated, cockade, heterogeneous morphology (Figure 31). These granules are of immature type, lamellated character being the result of incomplete aggregation of biogenic amines and glycosamino-glycans in specific granules. For these reasons, the evaluation of inflammatory infiltrate assumes the application of immunohistochemical methods specific to each cell type and the analysis of the report of the cell populations before and after the treatment.

Immunohistochemical evaluation of the inflammatory infiltrate

In order to assess the accuracy of immunohisto-chemical methods, the first method effectuated was vimentin, the specific antibody in V9 clone identifying the vast majority of cells of mesodermal origin. The intermediate filaments of vimentin are present both in the inflammatory infiltrate cells, as well as in the fix cells of the conjunctive tissue (Figure 32). The reaction does not have specificity for any of the cell populations, but is represents the positive marker of correct primary processing of specimens (fixing, inclusion). We have noticed the high density of the positive reaction for vimentin, especially at the cases with abundant inflammatory infiltrate, as seen in biopsies from treated patients (Figure 33).

Lymphocyte reaction

The heterogeneous nature of the inflammatory infiltrate determined us to approach the study of the lymphocyte population, which predominated in all cases before treatment. On sections stained with the usual methods, the lymphocytes were identified as round, small cells, with a similar nucleus, round and intensely colored. Cytoplasm was quantitatively reduced, so that in most cases it could not be observed. As stated above, nor the morphological methods, nor the histochemical ones do not allow differentiation between the two major classes of lymphocytes (B and T). To this purpose, we

performed immunohistochemical methods that highlight specific membrane antigens.

In the first place, we were preoccupied by the density and distribution of lymphocytes and for this reason we applied the method that reveals the leukocyte common antigen (LCA). LCA is a generic marker for lymphoid and macrophagic cells, expressed at the membrane level.

Before the treatment, we observed that almost all the cells in the inflammatory infiltrate are positive for LCA, which indicates that the main components are represented by the lymphocytes and macrophages. The reaction certifies fewer granulocytes and plasma cells, both negative for this antibody.

This reaction is not positive for conjunctive tissue cells, which facilitates the differentiation between mast cells and macrophages (Figure 34). B-lymphocytes were identified using the anti-CD20 antibody, whose epitope is expressed at membrane level (Figure 35).

Most of the lymphocytes from the inflammatory infiltrate were represented by positive cells for this antibody (Figure 36). As a particularity, we mention the fact that lymphocytes tended to dispose preferentially around small blood vessels in the immediate vicinity of the epithelium, under the basement membrane. In the same conditions, we noted the presence of a small number of T-lymphocytes, positive for immunoreactions to CD4 (Figure 37). Immunoreactions for CD3 and CD8 were negative in all cases.

After treatment, the residual inflammatory infiltrate consisted of positive B-lymphocytes for CD20, but dramatically reduced in number in comparison with the pretreatment phase (Figure 38), from a significantly increased number of CD4 positive T-lymphocytes (Figure 39) and numerous macrophages (Figure 40).

The macrophages were positive at the immuno-staining for CD68, macrophage-specific marker. The final product of the reaction was stained in brown, with granular cytoplasmic pattern (Figure 41). The black pigment observed on sections stained with routine methods was present in the cytoplasm of only a 10% of the total population of macrophages (Figure 42).

Figure 31 – *Fragment of cytoplasm of a mast cell with heterogeneous granules from an ultrastructural point of view. Lamellated granules with eccentric electron-dense condensation can be noticed, included in the cytoplasm with very rare non-specific organelles. Electron microscopy, ×52 000.*
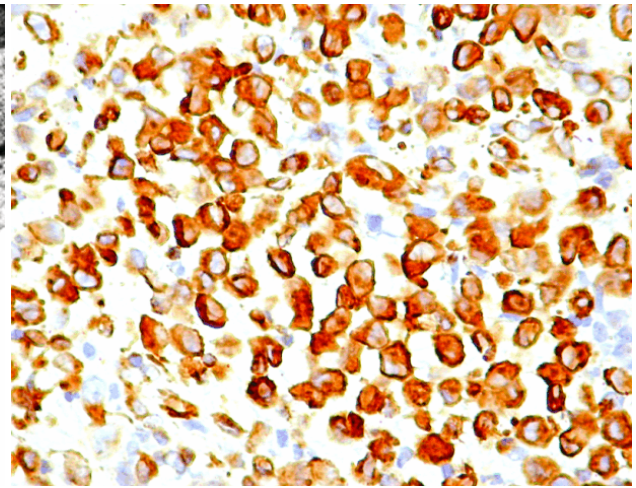

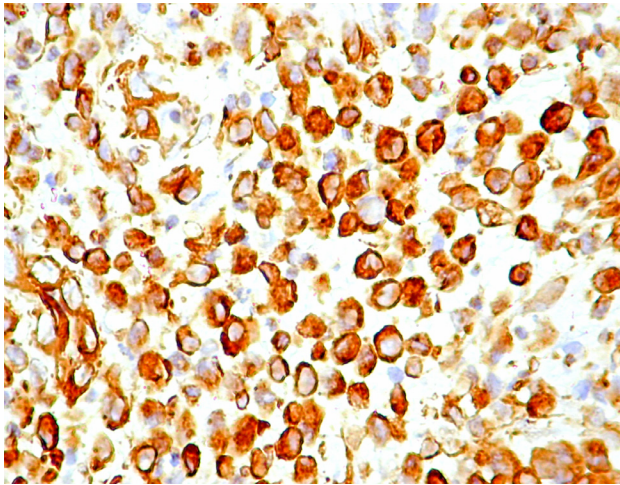**Figure 32 –** *Positive control: V9 vimentin (ob. ×20).*

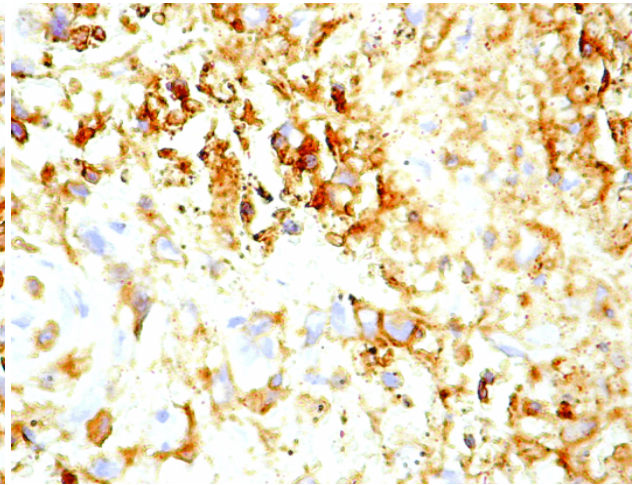**Figure 33 –** *Positive reaction to vimentin in the inflammatory infiltrate cells (ob. ×20).*

Figure 34 – *Positive immunoreactivity for LCA. The reduction of the intensity of reaction in the deep of lamina propria (ob. ×20).*
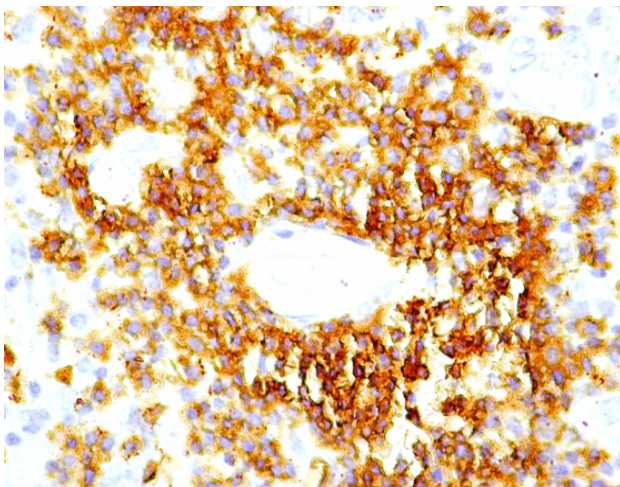

Figure 35 – *Positive immunoreactivity for CD20, the final reaction product membranary limited. The intensity of the reaction diminishes in the deep lamina propria, where positive lymphocytes and macrophages for the LCA are observed under the form of small or isolated groups (ob. ×20).*
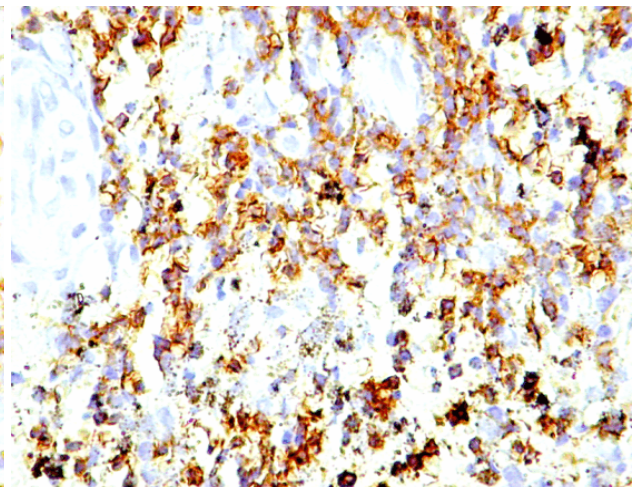

Figure 36 – *Numerous B-lymphocytes situated underneath the basement membrane (ob. ×20).*
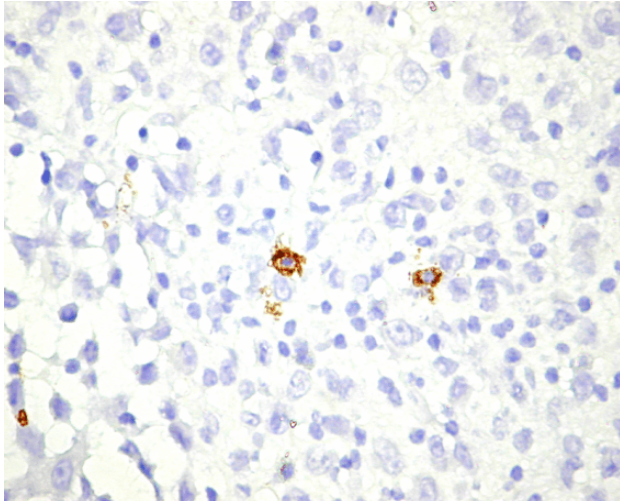
Figure 37 – *T-lymphocytes, CD4 positive (ob. ×20).*
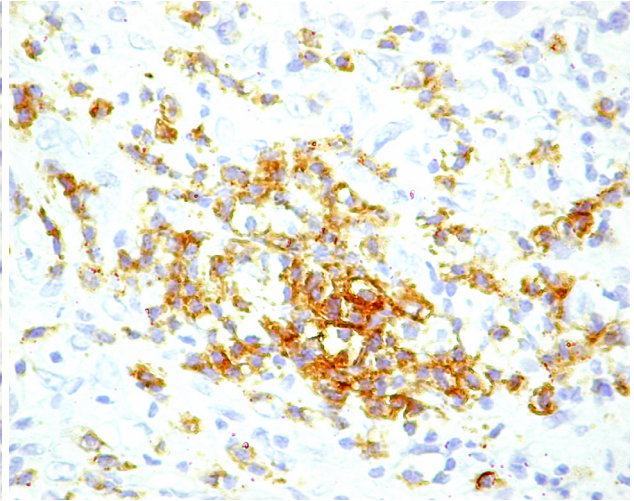
Figure 38 – *Immunoreaction for CD20, biopsy samples taken from the patient after treatment. There is a significantly lower number of positive cells compared with pretreatment biopsy (ob. ×20).*
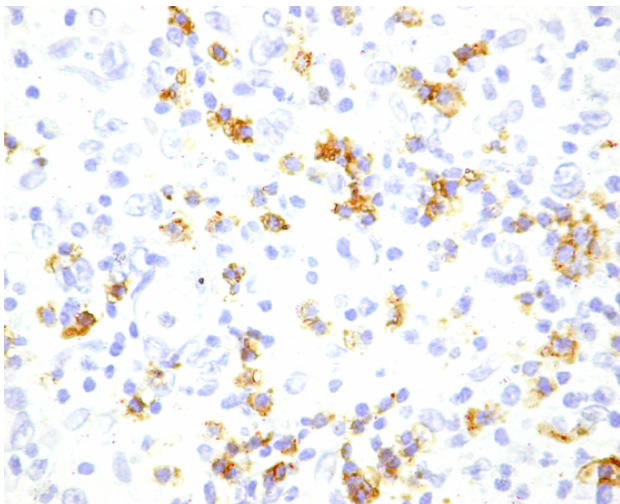
Figure 39 – *Immunoreaction for CD4. The cells are positive at the membrane, are arranged individually, significantly more numerous than in the pretreatment cases (ob. ×20).*

Figure 40 – *Positive immunoreaction for CD68: macrophage marker (ob. ×20).*

Figure 41 – *The final product of the reaction for CD68: cytoplasmic, granular (ob. ×20).*

Figure 42 – *CD68-positive macrophages, with and without pigment in the cytoplasm (ob. ×20).*

⬚ Discussion

The elaboration of an assessment, diagnosis and therapeutically behavior of the patient with chronic obstructive pulmonary disease protocol represents a major challenge in the next 10 years. Diagnosis is based o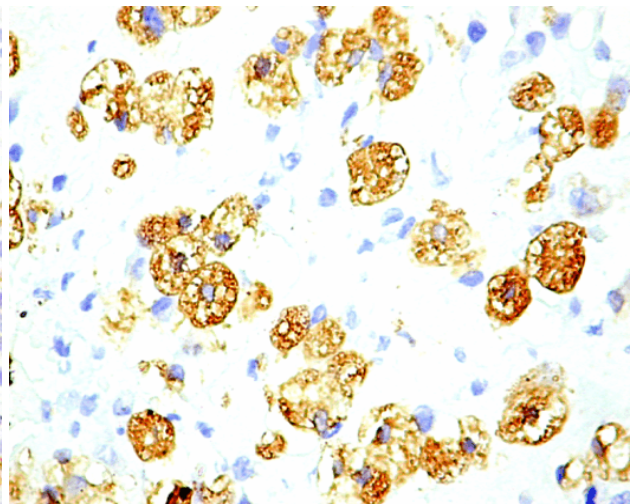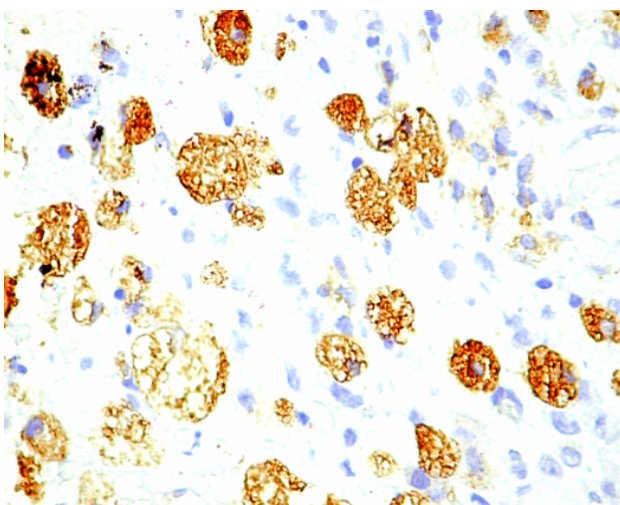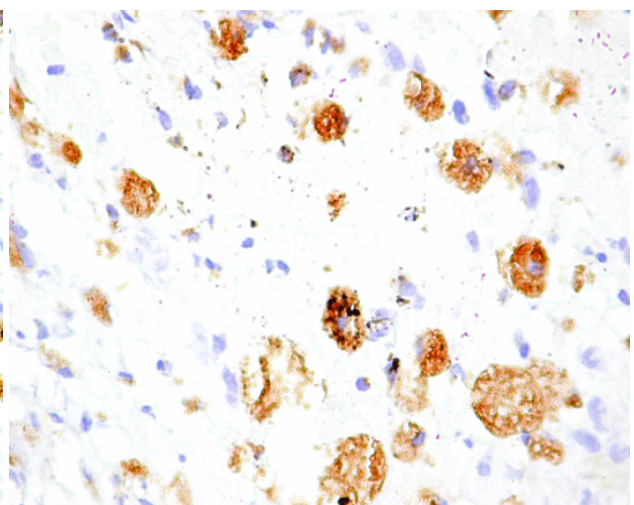n the history of exposure to risk factors, on demonstrating the airflow limitation (obstruction), on the presence of symptoms (chronic cough, chronic sputum production, dyspnea). Clinical signs of the obstructive lung syndrome occur later when the pulmonary function is significantly impaired, thus having a lower sensitivity and specificity in the diagnosis of COPD. Spirometry is "the gold standard" in confirming the diagnosis and assessing the severity of COPD. Classification of severity of COPD has an orientative role in the management of COPD, which in many cases is conducted depending on symptoms.

The airflow obstruction through bronchial pathways due to associating chronic bronchitis with pulmonary emphysema, defines chronic obstructive broncho-pneumopathy [10].

Chronic bronchitis and emphysema are two distinct processes, often present together in patients with chronic airways obstruction. Obstruction is:

▪ Chronic: the lower respiratory flow does not show significant changes during several months (which distinguish COPD from asthma). Generally irreversible, but sometimes partially reversible under the action of anticholinergic or β-adrenergic bronchodilator agents.

▪ Progressive: the natural evolution is slow to aggravation.

▪ Primitive: obstruction to flow is not generated by any disease with known etiopathogeny (bronchiectasis, cystic fibrosis, tuberculosis, sarcoidosis, silicosis, and cancer) [8].

Chronic bronchitis is associated with the hypertrophy of mucus-producing glands that are found in large, cartilaginous airway submucosa. In the small airways appear the hyperplasia of the muciparous cells, mucosal and submucosal inflammatory cells, edema, peribronchial fibrosis, intraluminal mucus plugs and smooth muscle hypertrophy. Alveolar epithelium is both the target and the initiation of inflammation in chronic bronchitis. Inflammation from bronchitis differs from the predominantly eosinophilic inflammation from asthma, due to the neutrophils and to the peribronchial location of fibrotic changes. The bronchial inflammation is the result of the action of IL8 and of variety of other chemotactic cytokines. Damaged epithelium can release small quantities of regulatory substances. The intensity of these inflammatory reactions correlates with bronchial reactivity in response to the action of toxic, infectious or inflammatory stimuli. Evidence regarding the increase of the number of neutrophils in the lungs at patients with emphysema is also controversial; many studies have involved alveolar macrophages as major cells producing inflammatory reactions. Di Stefano A *et al.* showed that an increased number of macrophages in bronchial biopsies correlate with airflow limitation. By comparison, the number of neutrophils was not increased, and there was no relationship between the number of neutrophils and the symptoms of the disease [11, 12].

Smoking is a major risk factor for developing COPD and cigarette smokers constitute over 90% of patients with COPD in developed countries. Recent studies performed on bronchial biopsies from patients with COPD have reported an increased infiltration of T-lymphocytes (CD3+ and CD8+ cells), macrophages and increased levels of chemotactic receptors CC5, in mild to moderate COPD. In addition, the inflammatory response in COPD is associated with increased expression of inflammatory proteins such as cytokines, chemokines 8 and adhesion molecules. Inflammatory changes that occur in COPD are also seen in cigarette smokers without COPD, but to a lesser extent [12].

In previous studies performed on COPD patients with moderate and mild forms, an increase in the number of T-lymphocytes and macrophages was observed. During exacerbations of COPD, there was an increase of the inflammatory cellular infiltrations and the repeated crises of viral or bacterial origin may induce a cascade of events resulting in induction and activation of cytokines and chemokines and the production of further inflammatory infiltrated cells. Unfortunately, a collection of bronchial biopsies from subjects during exacerbations is difficult to perform and rarely accepted by patients [13].

The clinical benefits associated with the use of inhaled therapy (BADLA, CIS), may be mediated, at least partially, through their anti-inflammatory efficacy, evaluated in the wall biopsies of airways. On short-term treatment of COPD, moderate form, the reduction of the inflammatory infiltrate was observed, but not also the reduction of bronchial CD8+ cells, neutrophils or macrophages. The long-term treatment evidentiated suppression effects of T-lymphocytes and of cells of bronchial inflammation [14].

The study aims to evaluate changes in bronchial mucosa, taken at endoscopy in patients with chronic obstructive pulmonary disease before and after administration of inhaled therapy. Morphological, histochemical and immunohistochemical evaluation, effectuated at untreated cases revealed the existence of severe lesions of the bronchial mucosa present in all its components.

In biopsies taken from treated patients, significant morphological changes from the initial biopsy were observed in eight cases (44%). These consisted in the restoration of the pseudostratified epithelium, increase in the number of mast cells with minimal or absent degranulations, reduction of the inflammatory infiltrate.

Challenges to be elucidated in the future in order to convince on the use of inhalatory corticotherapy in COPD, are essentially the following:

▪ Corticosteroids act by a direct effect on pro-inflammatory cells or indirectly on epithelial restoration or improvement of the reparatory mechanisms of the extracellular matrix;

▪ The existence of a mast inflammation in the periphery can be easier controlled with inhaled corticosteroids with small particles that enter at this level [15].

Chronic obstructive pulmonary disease remains a heterogeneous disease involving multiple risk factors, and the deepening of molecular and cellular mechanisms can generate more effective methods for early disease

detection, targeted pharmacotherapy and effective conduct in exacerbations.

⎗ Conclusions

The morphohistochemical and immunohistochemical analysis of biopsies taken before beginning the treatment revealed the following aspects:

▪ Degenerative alterations of the surface epithelium, loss of ciliary differentiation and the absence of caliciform cells, with hyperexfoliation and formation of pseudopapillary structures;

▪ Degenerative lesions of the glands associated with mucoid and oncocytic metaplasia;

▪ Presence of an important stasis in the dilated blood vessels, which have the wall partially hyalinized;

▪ Abundant chronic inflammatory infiltrate, with polymorphic character;

▪ The appearance of myofibroblasts in the deep area of lamina propria;

▪ Argyrophilic basement membrane present in all cases;

▪ Fragmentation and lysis of elastic fibers;

▪ Numerous degranulated mast cells associated to the inflammatory infiltrate with typical electron-dense granules;

▪ In the inflammatory infiltrate predominate CD20 positive B-lymphocytes, arranged particularly perivascular and in the vicinity of the basement membrane;

▪ Rare positive CD4 T-lymphocytes, which explains the low number of plasma cells;

After treatment, we observed the following aspects:

▪ Partial or complete regeneration of the covering epithelium in which cells with cilia differentiate and only occasionally appear caliciform cells;

▪ We did not notice regeneration processes at the glands in the lamina propria;

▪ Remaining myofibroblastic reaction in the lamina propria;

▪ Elastic fibers were not present after treatment;

▪ Increased number of mast cells with minimal or no degranulation, mast granules are of immature type, lamelled.

The immunohistochemical evaluation, together with the clinical and paraclinical evaluation constitutes a milestone in the initiation and evaluation of COPD therapy through the results obtained in evidentiating the structural changes before and after treatment, through morphological, histochemical and immunohistochemical study of biopsies taken by fibrobronchoscopy.

Applying therapeutic management principles on the study group was done with the help of the study that desires to demonstrate the beneficial role in the COPD therapy of combining a β2-agonist with an anticholinergic in order to obtain a supplementary bronchodilator effect administration, compared with the one corresponding to the administration of β2 agonist type bronchodilators.

Deepening the molecular and cellular mechanisms of COPD can lead to more effective methods for early detection of disease, targeted pharmacotherapy, and efficient conduct in exacerbations.

References

[1] Cato AC, Wade E, *Molecular mechanisms of anti-inflammatory action of glucocorticoids*, Bioessays, 1996, 18(5):371–378.

[2] Adams PF, Hendershot GE, Marano MA; Centers for Disease Control and Prevention/National Center for Health Statistics, *Current estimates from the National Health Interview Survey, 1996*, Vital Health Stat 10, 1999, (200):1–203.

[3] Akbari O, Freeman GJ, Meyer EH, Greenfield EA, Chang TT, Sharpe AH, Berry G, DeKruyff RH, Umetsu DT, *Antigen-specific regulatory T cells develop via the ICOS–ICOS-ligand pathway and inhibit allergen-induced airway hyper-reactivity*, Nat Med, 2002, 8(9):1024–1032.

[4] Anderson HR, Spix C, Medina S, Schouten JP, Castellsague J, Rossi G, Zmirou D, Touloumi G, Wojtyniak B, Ponka A, Bacharova L, Schwartz J, Katsouyanni K, *Air pollution and daily admissions for chronic obstructive pulmonary disease in 6 European cities: results from the APHEA project*, Eur Respir J, 1997, 10(5):1064–1071.

[5] Agustí AG, Carrera M, Barbé F, Muñoz A, Togores B, *Oxygen therapy during exacerbations of chronic obstructive pulmonary disease*, Eur Respir J, 1999, 14(4):934–939.

[6] Andersson F, Borg S, Jansson SA, Jonsson AC, Ericsson A, Prütz C, Rönmark E, Lundbäck B, *The costs of exacerbations in chronic obstructive pulmonary disease (COPD)*, Respir Med, 2002, 96(9):700–708.

[7] Bauldoff GS, Hoffman LA, Zullo TG, Sciurba FC, *Exercise maintenance following pulmonary rehabilitation: effect of distractive stimuli*, Chest, 2002, 122(3):948–954.

[8] Garcia-Aymerich J, Barreiro E, Farrero E, Marrades RM, Morera J, Antó JM, *Patients hospitalized for COPD have a high prevalence of modifiable risk factors for exacerbation (EFRAM study)*, Eur Respir J, 2000, 16(6):1037–1042.

[9] Ciurea T, *Respiratory diseases*, Medical University Publishing House, Craiova, 1996.

[10] ***, *Standards for the diagnosis and care of patients with chronic obstructive pulmonary disease. American Thoracic Society*, Am J Respir Crit Care Med, 1995, 152(5 Pt 2):S77–S121.

[11] Finlay GA, O'Driscoll LR, Russell KJ, D'Arcy EM, Masterson JB, Fitzgerald MX, O'Connor CM, *Matrix metalloproteinase expression and production by alveolar macrophages in emphysema*, Am J Respir Crit Care Med, 1997, 156(1):240–247.

[12] Di Stefano A, Caramori G, Oates T, Capelli A, Lusuardi M, Gnemmi I, Ioli F, Chung KF, Donner CF, Barnes PJ, Adcock IM, *Increased expression of nuclear factor-kappaB in bronchial biopsies from smokers and patients with COPD*, Eur Respir J, 2002, 20(3):556–563.

[13] Churg A, Dai J, Tai H, Xie C, Wright JL, *Tumor necrosis factor-alpha is central to acute cigarette smoke-induced inflammation and connective tissue breakdown*, Am J Respir Crit Care Med, 2002, 166(6):849–854.

[14] Suissa S, Barnes PJ, *Inhaled corticosteroids in COPD: the case against*, Eur Respir J, 2009, 34(1):13–16.

[15] Puchelle E, *Assembly Symposium: Regeneration and repair of airway epithelium. Mechanisms of airway epithelial repair and regeneration*, Program and Abstracts of the European Respiratory Society 12th Annual Meeting, September 14–18, 2002, Stockholm, Sweden.

Corresponding author
Gheorghe Nini, Teaching Assistant, MD, PhD, Clinical Department of Pneumology, "Vasile Goldiş" Western University Arad, 46 Mihai Eminescu Square, 310019 Arad, Romania; Phone +40744–764 498, e-mail: gheorghe.nini@yahoo.com